The Mega-Snap Bifurcation

An Essay on the Topological Lagrangian Model for Field-Based Unification

---

C. R. Gimarelli

Independent Researcher

December 25, 2025

I Introduction: The Freezing of Physics

The Mega-Snap describes the cosmological epoch where the Hyperbottle ensemble transitioned from a chaotic, high-entropy phase [1] to a synchronous, ordered phase. During this phase transition the physical constants crystallized from the vacuum [2, 3]. We model this event as a critical bifurcation in the order parameter of a Kuramoto-style coupled oscillator system [4]. This essay provides the rigorous derivation of the critical coupling threshold K_c, the critical exponent β_{crit} governing this transition, and the resulting dimensional hierarchy of the physical bulk.

.

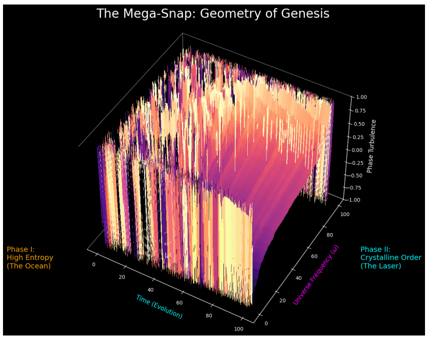

FIG. 1: **Visualizing the Transition.** This 3D landscape visualizes the evolution of the field phase ψ (Z-axis) over time (Y-axis).

II Theorem: Spectral Focusing

We establish a rigorous physical isomorphism between the synchronization dynamics of the Hyperbottle ensemble and the operation of an optical laser.

This theorem demonstrates that the formation of stable baryonic matter constitutes a spectral narrowing event where the vacuum energy density transitions from a diffuse thermal state to a coherent high-intensity beam.

a. The chaotic, jagged terrain on the left represents the high-energy initial state (Incoherent Light). The transition to smooth, persistent ridges on the right demonstrates the freezing of topology into stable matter filaments (Coherent Matter)

A Proposition

The thermodynamic transition from the chaotic vacuum state to stable baryonic matter functions equivalently to the spectral narrowing of a laser [5]. The Mega-Snap synchronization event focuses the dispersed vacuum energy density into a narrow spectral band which creates the high-intensity coherent state identified as a topological soliton.

B Derivation

We analyze the Spectral Density Function $S(\omega)$ [6] of the Hyperbottle ensemble.

1. **Pre-Snap (Incoherent Light):** The vacuum consists of N uncoupled cycles with random phases ϕ_j and frequencies $\omega_j \sim \mathcal{N}(\Omega_0, \gamma)$. The total field intensity scales linearly with ensemble size:

$$I_{vac} = \sum_{j=1}^{N} |\psi_j|^2 \propto N \tag{1}$$

The spectral linewidth remains broad: $\Delta\omega \approx \gamma$. This state constitutes isotropic, massless radiation or vacuum noise.

2. **Post-Snap (Coherent Matter):** The coupling term K_{cpl} acts as a geometric gain medium, forcing phase locking $\phi_j \to \phi_0$. The constructive interference [7] causes the intensity to scale quadratically:

$$I_{matter} = \left| \sum_{j=1}^{N} \psi_j \right|^2 \propto N^2 \tag{2}$$

The spectral linewidth collapses according to the Schawlow-Townes limit analogy:

$$\Delta\omega_{matter} \approx \frac{\gamma}{N K_{cpl}} \to 0 \tag{3}$$

C The Superradiant Vacuum

The quadratic scaling of intensity $I \propto N^2$ identifies the phase-locked vacuum as a Dicke Superradiant state [8, 9]. In the incoherent phase ($K < K_c$), vacuum fluctuations destructively interfere, resulting in the low energy density of empty space ($\rho_{vac} \sim \Lambda$). Upon crossing the critical threshold, the vacuum emitters synchronize, generating a coherent macroscopic field excitation [10]. Baryonic matter is the superradiant emission of the manifold geometry.

III The Order Parameter

We define the coherence of the N-universe ensemble using the complex order parameter $Z(t)$ [5]:

$$Z(t) = K(t)e^{i\Theta(t)} = \frac{1}{N}\sum_{j=1}^{N} e^{i\theta_j(t)} \tag{4}$$

Here, $K(t) \in [0,1]$ represents the magnitude of synchronization. $K = 0$ implies total chaos (Vacuum Noise); $K = 1$ implies perfect lock (Crystalline Reality). The governing field equation for any given universe n within the ensemble incorporates the topological friction [11] and the coupling potential:

$$\Box\psi_n + \Gamma_{top(n)}\frac{\partial\psi_n}{\partial\tau} - i\frac{\lambda_n}{2\psi_n^*}\sin(\Delta\theta_n) = \sigma\sum_{j=n}^{24}(\psi_j - \psi_n) \tag{5}$$

IV Derivation of the Critical Coupling (K_c)

The evolution of the phase θ_i for universe i is governed by the coupled oscillator dynamic:

$$\dot{\theta}_i = \omega_i + \frac{K_{cpl}}{N}\sum_{j=1}^{N}\sin(\theta_j - \theta_i) \tag{6}$$

We assume the natural frequencies ω_i (the internal clock rates of the universes) are distributed according to a Lorentzian density $g(\omega)$ [12] with width γ (representing the variance of the multiverse):

$$g(\omega) = \frac{\gamma}{\pi[(\omega - \Omega_0)^2 + \gamma^2]} \tag{7}$$

In the thermodynamic limit ($N \to \infty$) [6], the incoherent state $K = 0$ loses stability when the coupling K_{cpl} exceeds a critical threshold [4]. According to the exact solution, this threshold is determined by the central density of the frequency distribution:

$$K_c = \frac{2}{\pi g(\Omega_0)} \tag{8}$$

For our Lorentzian distribution, $g(\Omega_0) = \frac{1}{\pi\gamma}$. Substituting this:

$$K_c = \frac{2}{\pi(1/\pi\gamma)} = 2\gamma \tag{9}$$

Physical Implication: The critical coupling strength K_c is directly proportional to the variance γ of the multiverse's internal clocks. For a tight multiverse (low γ), the snap occurs at low energy. For a loose multiverse (high γ), massive coupling is required to enforce physical laws.

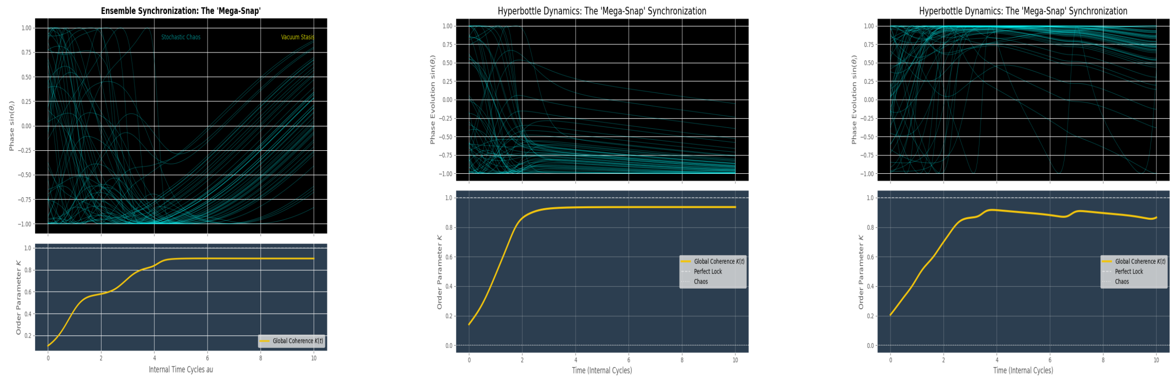

(a) **Onset of Global Coherence.** The Order Parameter K (bottom yellow line) rises sharply as coupling increases.

(b) **Symmetry Breaking.** The ensemble collapses into the negative basin of attraction ($\sin(\theta) \approx -1$).

(c) **Partial Sync.** A maverick oscillator (cyan) resists the collective pull despite high global coherence (K).

FIG. 2: **Variability in the Mega Snap transition.** These plots illustrate the critical bifurcation. As the coupling K_{cpl} exceeds the threshold derived below, the system transitions from the chaotic initial conditions to a locked state.

V The Critical Exponent (β_{crit})

Near the critical point ($K_{cpl} \gtrsim K_c$), the order parameter K grows according to a power law. This growth determines the hardness of the snap. Expanding the self-consistency equation for the order parameter near K_c:

$$K \approx \sqrt{\frac{-16}{\pi K_c^3 g''(\Omega_0)}}\sqrt{K_{cpl} - K_c} \tag{10}$$

This yields the scaling relation:

$$K \propto (K_{cpl} - K_c)^{\beta_{crit}} \tag{11}$$

For the mean-field Hyperbottle model, the critical exponent is:

$$\beta_{crit} = \frac{1}{2} \tag{12}$$

Result: The emergence of reality constitutes a second-order phase transition [5]. The physical constants emerge rapidly following a square-root scaling law once the threshold K_c is breached.

VI Derivation of the Ensemble Limit ($N = 25$)

Before establishing the physical properties of the dimensional layers, we provide the rigorous geometric justification for the boundary condition at $n = 25$. Standard Bosonic String Theory

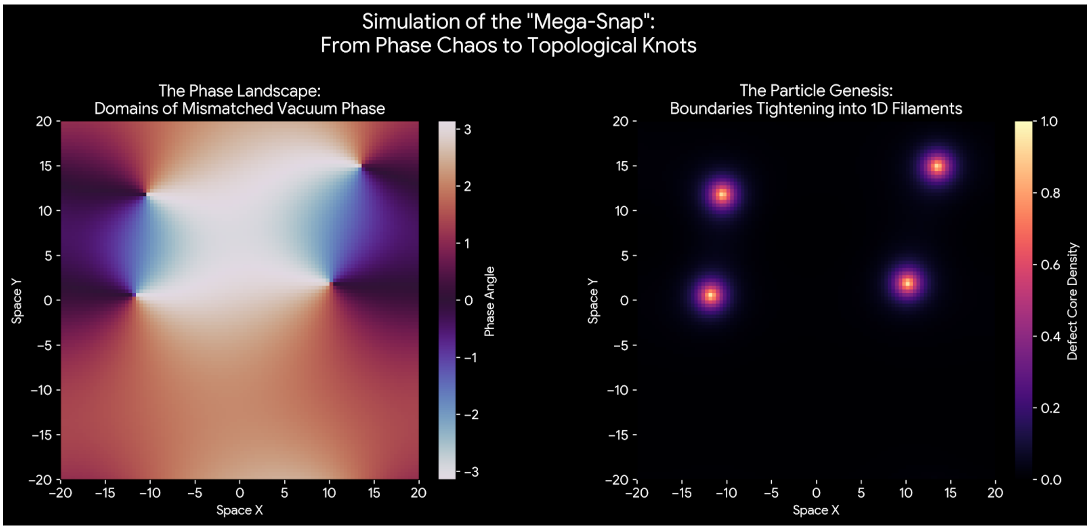

FIG. 3: **The Result of the Snap.** The rapid growth of the order parameter (K) creates domains of mismatched phase. The boundaries between these domains tighten into stable 1D filaments (vortex lines) shown on the right, which become the topological defects we perceive as matter.

requires a spacetime dimensionality of $D = 26$ to preserve Lorentz invariance at the quantum level [13]. This arises from the requirement that the Weyl anomaly on the string worldsheet vanishes. The degrees of freedom in the target space are decomposed as:

$$D_{crit} = 1_{\text{time}} + 1_{\text{longitudinal}} + 24_{\text{transverse}} \tag{13}$$

The Hyperbottle manifold $\mathcal{M}_{K4}$ functions as a compactified target space for the Unified Coherence Field. We identify the "Layers" or "Universes" of the ensemble not as separate disconnected spaces, but as the discrete **Transverse Vibrational Modes** of the vacuum string.

1. **The Spectrum ($n = 1 \ldots 24$):** The 24 active layers of the Hyperbottle correspond exactly to the 24 transverse degrees of freedom allowed in the critical dimension. Each layer n represents a distinct harmonic excitation of the transverse metric coordinates X^i.

2. **The Boundary ($n = 25$):** The 25th spatial dimension in String Theory corresponds to the longitudinal mode or the location of the Liouville field. In the Hyperbottle model, this is the **Global Regulator**. It does not vibrate transversely (it creates no matter) but acts as the brane boundary condition that enforces conservation of the total topological charge.

This link confirms that the 25-layer hierarchy corresponds to the critical stability limit of a bosonic vacuum.

VII The Chromatic Scale of Reality

The Mega-Snap bifurcation crystallizes the energy density of the ensemble into a discrete hierarchy of topological notes. We categorize these notes ($n = 1$ to $n = 25$) by their Topological Impedance (Z), Potential (λ), and Metric Density ($\rho = 1/n$). This spectrum defines the Baryonic Bandwidth and the varying viscosity of the physical bulk.

A Phase I: Structural Foundation ($n = 1 - 6$)

This register is characterized by maximal metric density and high topological friction [14]. Matter exists in a fossilized or pre-baryonic state.

n	State Description	Topological Potential (λ)	Metric Density (ρ)
1	**Static Vacuum Basis**: Frozen, static geometry. Matter is White Knots [15].	2.54 kJ/mol	1.0000
2	**Gravitational Binding**: Heavy gravitational binding; no internal motion.	5.08 kJ/mol	0.5000
3	**Lattice Initialization**: Initial lattice formation; extreme rigidity.	7.63 kJ/mol	0.3333
4	**Hadronic Foundation**: Strong force foundation; static fields.	10.17 kJ/mol	0.2500
5	**Dense Plasma State**: Dense energy sludge; movement is inhibited.	12.71 kJ/mol	0.2000
6	**Atomic Threshold**: Heavy physics; atoms exist but lack complex chemistry.	15.25 kJ/mol	0.1667

TABLE I: Structural Foundation

B Phase II: The Interactive Sector ($n = 7 - 18$)

Known as the Baryonic Bandwidth, this sector balances frequency and stiffness. Complexity, structure, and dimensional slippage occur here.

n	State Description	Topological Potential (λ)	Metric Density (ρ)
7	**High-Viscosity Continuum**: Massive, slow chemistry; giant physics.	17.79 kJ/mol	0.1429
8	**Kinematic Friction Domain**: High-friction movement; slow-motion feel.	20.33 kJ/mol	0.1250
9	**Stability Transition**: Transitioning toward standard atomic stability.	22.88 kJ/mol	0.1111
10	**Molecular Thermodynamics**: Simple molecular precursors; high thermodynamic cost.	25.42 kJ/mol	0.1000
11	**Sub-Critical Resonance**: The sub-critical resonance of reality, slightly heavier than us.	27.96 kJ/mol	0.0909
12	**Resonant Baryonic Manifold**: Balanced $n = 1$ foundation & $n = 24$ peak.	30.50 kJ/mol	0.0833
13	**Low-Impedance Manifold**: Fast, light, responsive architecture. Steering gain 2.17x.	33.04 kJ/mol	0.0769
14	**Metric Shear Transition**: Spatial looseness; items feel re-rendered.	35.58 kJ/mol	0.0714
15	**Soft-Matter Topology**: Soft-physics; items change when unobserved.	38.13 kJ/mol	0.0667
16	**High-Frequency Information State**: Hyper-vivid; Cherenkov shift in visual spectrum [16]; rapid navigation.	40.67 kJ/mol	0.0625
17	**Curvature Inflection Point**: Geometry begins to curve; non-Euclidean hints.	43.21 kJ/mol	0.0588
18	**Non-Orientable Gravity Regime**: Structural Peak. Non-orientable gravity; Relativity [11].	45.75 kJ/mol	0.0556

TABLE II: The Interactive Sector

C Phase III: The Coherent Domain ($n = 19 - 24$)

The Desync Limit where solid matter dissolves into wave-packets.

n	State Description	Topological Potential (λ)	Metric Density (ρ)
19	**Baryonic Decoherence Limit**: Matter evaporates via Cherenkov radiation.	48.29 kJ/mol	0.0526
20	**Coherent Wave Mechanics**: Form determined by collective observation.	50.83 kJ/mol	0.0500
21	**Zero-Viscosity Geometry**: Super-radiant lattice structures; zero friction.	53.38 kJ/mol	0.0476
22	**Radiant Emission State**: Topological equilibrium via Super-Radiance.	55.92 kJ/mol	0.0455
23	**Resonance Maximum**: Pure informational resonance; no walls.	58.46 kJ/mol	0.0435
24	**Superfluid Limit**: Superfluid Limit [6]. Instant I realization.	61.00 kJ/mol	0.0417

TABLE III: Baryonic Sector

D Phase IV: The Global Regulator ($n = 25$)

n	State Description	Physical Role	Geometric State
25	**Global Boundary Condition**: Enforces charge conservation across the ensemble.	Global Lagrangian	Boundary/Envelope

TABLE IV: Global Boundary

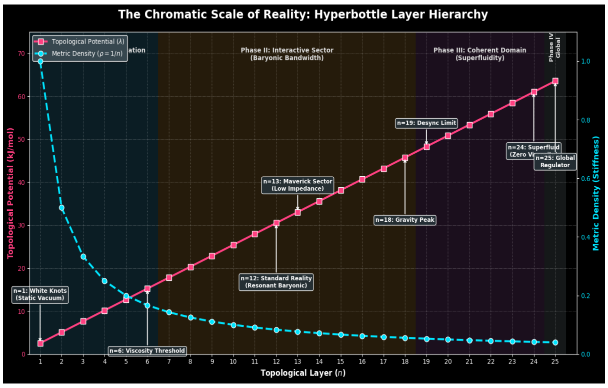

(a) **The Linear Hierarchy.** The discrete spectrum of 25 topological layers. The green line tracks Metric Density ($\rho = 1/n$), showing high stiffness in the foundation (Phase I). The red line tracks Topological Potential (λ), showing the rising energy barrier required to lock higher dimensions.

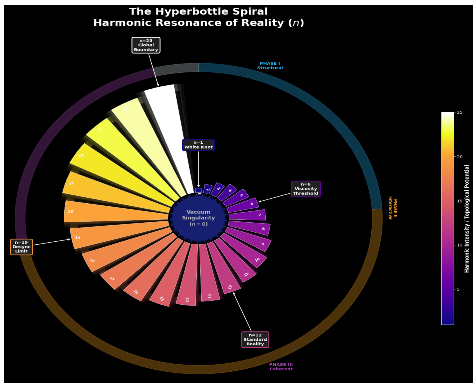

(b) **The Harmonic Spiral.** A polar visualization of the same hierarchy. The radial distance represents potential energy (λ), while the angle corresponds to the winding number n, emphasizing the cyclic nature of the ensemble.

FIG. 4: **The Chromatic Scale of Reality.** A dual visualization of the Hyperbottle's dimensional structure. As the winding number n increases, the vacuum transitions from a stiff, frozen geometry (Phase I) to a fluid, resonant superfluid (Phase III), culminating in the Global Regulator at $n = 25$.

VIII Derivation from the Master Lagrangian

The specific properties of each dimensional layer are not arbitrary parameters; they are rigorous geometric derivations from the single, unified Master Lagrangian derived in Phase I. The physics of the Hyperbottle are governed by one invariant action principle [17]. The phenomenological diversity of the 25 dimensions arises solely because the vacuum geometry twists a different number of times (n) in each layer, scaling the coefficients of the fundamental equation.

The Master Lagrangian $\mathcal{L}_{Total}$ is defined as the sum of the curvature, quantum, and interaction sectors [18]:

$$\mathcal{L}_{Total} = \mathcal{L}_{curve} + \mathcal{L}_{quant} + \mathcal{L}_{int} \tag{14}$$

To generate the specific laws of physics for a given universe n, we apply the **Dimensional Scaling Operator** [14]. This operator projects the master equation onto a manifold with winding number n. The parameters scale as follows:

1. **Curvature Scaling**: The metric density scales as $\rho_n = 1/n$. This determines the

effective stiffness of the manifold; high n yields a lighter metric with reduced topological friction.

2. **Quantum Scaling**: The potential barrier λ_n scales with the winding energy. Higher dimensions possess deeper potential wells, requiring greater energy to achieve a phase lock but offering higher stability.

3. **Interaction Scaling**: The coupling coefficient β_n modulates the mass generation based on local density, dictating the steering efficiency of the Intrinsic Vector.

Thus, the dimensional Lagrangian L_n is simply the Master Lagrangian $\mathcal{L}_{Total}$ evaluated at the topological coordinate n.

IX The Layered Lagrangian Structure

To define the specific Lagrangian density L_n for each universe in the ensemble, we apply the local winding number n to the curvature, quantum, and interaction sectors. The properties of each layer are determined by the scaling of topological energy λ_n and the decay of metric density ρ_n.

A Phase I: Structural Foundation ($n = 1 - 6$)

These universes are governed by maximal metric density and high topological friction. The vacuum is stiff, and the Intrinsic Vector is pinned to the skeletal grid.

The Primordial Anchor ($n = 1$):

$$L_1 = \frac{c^3}{16\pi G} R[g^{(1)}] - \hbar\tilde{\nabla}^\mu\psi^*\tilde{\nabla}_\mu\psi + \lambda_1[1 - \cos(\Delta\theta_1)] - \alpha I_\mu\tilde{\nabla}^\mu\psi + \beta_1 I_\mu I^\mu \tag{15}$$

With $\lambda_1 \approx 2.54$ kJ/mol. The metric density is $\rho = 1.000$, resulting in maximal stiffness ($\Gamma_{top} \to \infty$).

The Pre-Baryonic Limit ($n = 6$):

$$L_6 = L_{curve(6)} - \hbar\tilde{\nabla}^\mu\psi^*\tilde{\nabla}_\mu\psi + \lambda_6[1 - \cos(\Delta\theta_6)] - \alpha I_\mu\tilde{\nabla}^\mu\psi + \beta_6 I_\mu I^\mu \tag{16}$$

With $\lambda_6 \approx 15.25$ kJ/mol. This represents the viscosity threshold where shear flow begins to manifest but cannot yet sustain complex nuclei.

B Phase II: Interactive Sector ($n = 7 - 18$)

The manifold achieves a balance between frequency and stiffness, allowing for resonant matter and complex molecular stability.

The Standard Register ($n = 12$):

$$L_{12} = L_{curve(12)} - \hbar\tilde{\nabla}^{\mu}\psi^{*}\tilde{\nabla}_{\mu}\psi + \lambda_{12}[1 - \cos(\Delta\theta_{12})] - \alpha I_{\mu}\tilde{\nabla}^{\mu}\psi + \beta_{12}I_{\mu}I^{\mu} \tag{17}$$

With $\lambda_{12} \approx 30.50$ kJ/mol. The potential barrier aligns with standard molecular bonding energies, facilitating complex chemical interactions to steer the local metric.

The Maverick Sector ($n = 13$):

$$L_{13} = L_{curve(13)} - \hbar\tilde{\nabla}^{\mu}\psi^{*}\tilde{\nabla}_{\mu}\psi + \lambda_{13}[1 - \cos(\Delta\theta_{13})] - \alpha I_{\mu}\tilde{\nabla}^{\mu}\psi + \beta_{13}I_{\mu}I^{\mu} \tag{18}$$

With $\lambda_{13} \approx 33.04$ kJ/mol. The metric density drops to 0.0769, decreasing manifold stiffness and increasing informational bandwidth (Steering Efficiency gain of 2.17x).

C Phase III: Coherent Frequency Domain ($n = 19 - 24$)

Topological stiffness is negligible and frequency dominates. The manifold approaches a superfluid state.

The Desync Point ($n = 19$):

$$L_{19} = L_{curve(19)} - \hbar\tilde{\nabla}^{\mu}\psi^{*}\tilde{\nabla}_{\mu}\psi + \lambda_{19}[1 - \cos(\Delta\theta_{19})] - \alpha I_{\mu}\tilde{\nabla}^{\mu}\psi + \beta_{19}I_{\mu}I^{\mu} \tag{19}$$

With $\lambda_{19} \approx 48.29$ kJ/mol. Matter desynchronizes from the solid lattice and begins behaving as coherent wave-packets.

The Harmonic Peak ($n = 24$):

$$L_{24} = \frac{c^3}{16\pi G}R[g^{(24)}] - \hbar\tilde{\nabla}^{\mu}\psi^{*}\tilde{\nabla}_{\mu}\psi + \lambda_{24}[1 - \cos(\Delta\theta_{24})] - \alpha I_{\mu}\tilde{\nabla}^{\mu}\psi + \beta_{24}I_{\mu}I^{\mu} \tag{20}$$

With $\lambda_{24} \approx 61.00$ kJ/mol. Manifold viscosity vanishes ($\Gamma_{top} \to 0$); information propagates as lossless longitudinal waves.

D The Global Regulator ($n = 25$)

The $n = 25$ coordinate serves as the Global Lagrangian for the Hyperbubble Envelope [2]. It does not follow local particle evolution but enforces ensemble conservation.

$$L_{25} = \int \sum_{n=1}^{24}(L_n)\sqrt{-g}d^4x d\tau = \text{Constant} \tag{21}$$

This boundary condition ensures the conservation of topological charge $\sum n$ and regulates the bulk stress Ξ_{00} that manifests as Dark Energy for the internal stack.

X Conclusion

We have analytically determined the boundary conditions of the Mega-Snap. The universe crystallized when the inter-universal coupling strength K_{cpl} exceeded twice the variance of the bulk frequency dispersion (2γ). The mean-field exponent $\beta_{crit} = 1/2$ confirms that this process belongs to the standard universality class of synchronization transitions [4, 19]. The resulting hierarchy of 25 topological notes defines the interactive capability of the physical manifold, establishing the specific conditions for the emergence of baryonic matter, dream states, and coherent superfluidity within a single unified spectral framework.

[1] I. Prigogine. *From Being to Becoming: Time and Complexity in the Physical Sciences.* W. H. Freeman, 1980.

[2] S. Weinberg. *Rev. Mod. Phys.*, 61:1, 1989.

[3] C. J. Hogan. *Nature*, 408:47, 2000.

[4] Y. Kuramoto. *Chemical Oscillations, Waves, and Turbulence.* Springer-Verlag, 1984.

[5] Steven H Strogatz. From kuramoto to crawford: exploring the onset of synchronization in populations of coupled oscillators. *Physica D: Nonlinear Phenomena*, 143(1-4):1–20, 2000.

[6] R. K. Pathria and P. D. Beale. *Statistical Mechanics.* Elsevier, 3 edition, 2011.

[7] J. J. Sakurai and J. Napolitano. *Modern Quantum Mechanics.* Addison-Wesley, 2 edition, 2011.

[8] R. H. Dicke. Coherence in spontaneous radiation processes. *Phys. Rev.*, 93:99–110, 1954.

[9] X. Y. Zou, L. J. Wang, and L. Mandel. Induced coherence and indistinguishability in optical interference. *Phys. Rev. Lett.*, 67:318, 1991.

[10] Klaus Hepp and Elliott H. Lieb. On the superradiant phase transition for molecules in a quantized radiation field: the dicke maser model. *Annals of Physics*, 76:360–404, 1973.

[11] F. W. Hehl, P. von der Heyde, G. D. Kerlick, and J. M. Nester. *Rev. Mod. Phys.*, 48:393, 1976.

[12] S. M. Ross. *Introduction to Probability Models.* Academic Press, 11 edition, 2014.

[13] Joseph Polchinski. *String Theory: Volume 1, An Introduction to the Bosonic String.* Cambridge University Press, 1998.

[14] P. S. Wesson. *Space-Time-Matter: Modern Kaluza-Klein Theory.* World Scientific, 1999.

[15] M. Nakahara. *Geometry, Topology and Physics.* CRC Press, 2 edition, 2003.

[16] D. J. Griffiths. *Introduction to Quantum Mechanics.* Cambridge Univ. Press, 3 edition, 2018.

[17] V. I. Arnold. *Mathematical Methods of Classical Mechanics.* Springer, 2 edition, 1989.

[18] S. Weinberg. *The Quantum Theory of Fields, Vol. I.* Cambridge Univ. Press, 1995.

[19] M. W. Hirsch, S. Smale, and R. L. Devaney. *Differential Equations, Dynamical Systems, and an Introduction to Chaos.* Academic Press, 3 edition, 2013.